nature microbiology

ARTICLES

https://doi.org/10.1038/s41564-018-0160-4

Cryptococcus neoformans sexual reproduction is controlled by a quorum sensing peptide

Xiuyun Tian[1,7], Guang-Jun He[1,7], Pengjie Hu[1,2,7], Lei Chen[1,2], Changyu Tao[3], Ying-Lu Cui[4], Lan Shen[1], Weixin Ke[1,2], Haijiao Xu[1], Youbao Zhao[5], Qijiang Xu[6], Fengyan Bai[1], Bian Wu[4], Ence Yang[3], Xiaorong Lin[5] and Linqi Wang[1,2*]

Bacterial quorum sensing is a well-characterized communication system that governs a large variety of collective behaviours. By comparison, quorum sensing regulation in eukaryotic microbes remains poorly understood, especially its functional role in eukaryote-specific behaviours, such as sexual reproduction. *Cryptococcus neoformans* is a prevalent fungal pathogen that has two defined sexual cycles (bisexual and unisexual) and is a model organism for studying sexual reproduction in fungi. Here, we show that the quorum sensing peptide Qsp1 serves as an important signalling molecule for both forms of sexual reproduction. Qsp1 orchestrates various differentiation and molecular processes, including meiosis, the hallmark of sexual reproduction. It activates bisexual mating, at least in part through the control of pheromone, a signal necessary for bisexual activation. Notably, Qsp1 also plays a major role in the intercellular regulation of unisexual initiation and coordination, in which pheromone is not strictly required. Through a multi-layered genetic screening approach, we identified the atypical zinc finger regulator Cqs2 as an important component of the Qsp1 signalling cascade during both bisexual and unisexual reproduction. The absence of Cqs2 eliminates the Qsp1-stimulated mating response. Together, these findings extend the range of behaviours governed by quorum sensing to sexual development and meiosis.

Sexual reproduction is a universal feature in eukaryotes, including fungi[1–3]. One of the model organisms used to study sexual reproduction is the prevalent human fungal pathogen *Cryptococcus neoformans*. *C. neoformans* has two sexual reproduction forms: bisexual reproduction, taking place between cells of two compatible mating types (α and **a**), and unisexual reproduction (also termed haploid fruiting), involving only cells of the same mating type (mostly α)[4]. Like *C. neoformans*, its sibling pathogen *Cryptococcus gattii* has also been revealed to be able to undergo both bisexual and unisexual mating[5]. Previous observations have indicated a global dominance by α isolates in both *C. neoformans* and *C. gattii*[6]. This severe bias towards the α mating type probably leads to an infrequence of bisex in nature and mirrors the significance of α unisex in these pathogens. Developmentally, bisex and unisex undergo similar sequential differentiation processes, including filamentation, basidial formation, meiosis and sporulation[7]. However, these two sexual cycles can be differentiated by certain cellular events or morphological features. For instance, cell–cell fusion (syngamy) is essential for the generation of dikaryotic hyphae during bisexual development, and these filaments have special fused clamp cells[7]. By comparison, filaments are monokaryotic and clamp cells are unfused during unisexual reproduction, in which endo-replication or cell fusion-independent karyogamy events but not syngamy are presumed the major approaches for ploidy change[7,8].

The mating MAPK cascade is the major signalling pathway for both bisex and unisex[9,10], and many components of this pathway, such as HMG regulator Mat2, are required for both reproduction modes. Their disruption not only abolishes or substantially impairs **a**–α cell fusion during bisex but also prevents monokaryotic filamentation (also termed self-filamentation) during haploid fruiting[11,12]. In contrast, some upstream components critical for the paracrine induction of bisex (Fig. 1a), including α pheromone Mfα, G protein-coupled receptor Ste3α and pheromone transporter Ste6, appear to be not strictly required for unisexual mating. The corresponding mutants in the JEC21α background (*mf1,2,3*αΔ, *ste3*αΔ and *ste6*Δ) have been found to be severely defective in bisexual mating but to retain partial or full capability to undergo self-filamentation[13–16]. This led us to ask whether other paracrine systems contribute to the activation and coordination of the *Cryptococcus* unisexual cycle.

Results

The mating pheromone Mfα is largely dispensable for unisexual initiation and coordination in XL280α. We first deleted all three pheromone genes and generated the pheromoneless mutant (*mf1,2,3*αΔ) in XL280α, which was chosen in the study because of its well-described ability to undergo robust unisexual development[17]. This aspect enabled us to sensitively assess various phases during the unisexual cycle in this mutant. We showed that the absence of the mating pheromone in XL280α did not result in evident impairment in the sequential differentiation events associated with unisexual development, including self-filamentation and sporulation (Fig. 1b–c). Consistently, the absence of the pheromone Mfα only slightly affected the expression of the extracellular matrix signal Cfl1, a filament-specific molecular indicator[18,19], which was nearly undetected in the *mat2*Δ mutant (Fig. 1d). In contrast,

[1]State Key Laboratory of Mycology, Institute of Microbiology, Chinese Academy of Sciences, Beijing, China. [2]University of Chinese Academy of Sciences, Beijing, China. [3]Department of Microbiology, School of Basic Medical Sciences, Peking University Health Science Center, Beijing, China. [4]CAS Key Laboratory of Microbial Physiological and Metabolic Engineering, Institute of Microbiology, Chinese Academy of Sciences, Beijing, China. [5]Department of Microbiology, University of Georgia, Athens, GA, USA. [6]College of Life Science, Northeast Forestry University, Harbin, China. [7]These authors contributed equally to this work: Xiuyun Tian, Guang-Jun He, Pengjie Hu. *e-mail: wanglq@im.ac.cn

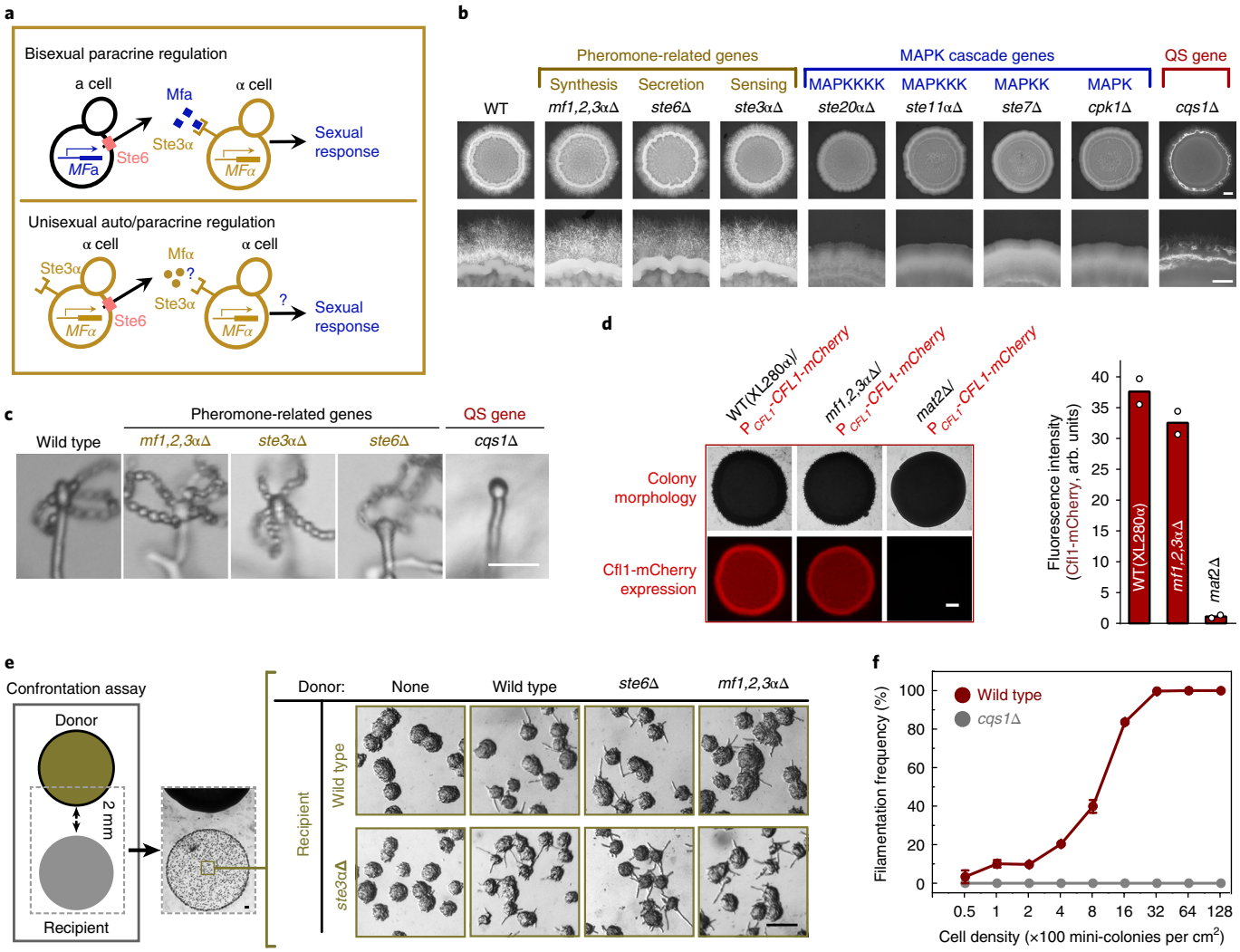

Fig. 1 | The mating pheromone is largely dispensable for unisexual reproduction in the XL280α background. a, Schematic diagram depicting proposed pheromone auto/paracrine regulation during bisexual and unisexual mating, respectively. During bisexual mating, the pheromone Mf**a** is produced by **a** cells, in which the transporter Ste6 facilitates its secretion. Secreted pheromone strongly induces mating response by binding to the compatible GPCR receptor Ste3α of α cells[9,13]. The compatibility of Mfα and Ste3α during α unisexual reproduction remains unclear. **b**, The effect of the absence of various components of mating MAPK signalling and the *CQS1* gene on aerial hyphal morphogenesis at the colony level during unisexual development. MAPK, the mitogen-activated protein kinase (Cpk1); MAPKK, MAPK kinase (Ste7); MAPKKK, MAPK kinase kinase (Ste11α); MAPKKKK, MAPK kinase kinase kinase (Ste20α); QS, quorum sensing; WT, wild type. The hyphae in different strains were photographed after 10 days of growth. Scale bars, 1 mm. **c**, The effect of the absence of components of pheromone signalling and the *CQS1* gene on sporulation during unisexual development. The spore chains in different strains were photographed after 1 week of growth. Scale bar, 20 μm. **d**, Pheromone is not required for expression of Cfl1 during unisexual reproduction based on images (left) and quantification of fluorescence intensity (right). Graph shows mean fluorescence intensity of two colonies for each strain. Arb., arbitrary. Scale bar, 1 mm. **e**, Diagram shows quantitative analysis method for paracrine induction of unisex based on the confrontation assay (left). Recipient strain was dropped in proximity to pre-incubated donor colony and incidence of forming filamentous mini-colonies in recipient strain was recorded. The mini-colonies in different recipient strains were photographed 16 h after inoculation of the recipient (right). Scale bars, 100 μm. **f**, Cells of XL280α and the *cqs1*Δ mutant were plotted on mating-inducing medium (V8 agar) at different concentrations. Filamentation frequency was calculated based on the percentage of filamentous mini-colonies 21 h after mating induction. $n = 3$ independent experiments, mean ± s.e.m. In **b**,**c**,**e**, images are representative of more than five independent experiments conducted with similar results.

self-filamentation in XL280α was not observed in the mutants disrupting the gene encoding the downstream MAPK cascades (Fig. 1b). This echoes the phenotypes observed in the JEC21α -derived counterpart mutants[11].

Quorum sensing peptides induce unisex. We next sought to examine whether there is another intercellular communication system that could induce unisex in *C. neoformans*. For this, we used a quantitative approach based on confrontation analysis to evaluate the stimulatory effect by the potential unisex-inducing signal (Fig. 1e). We found that neither the absence of Mfα in the donor nor mutating *STE3*α in the recipient can attenuate the intercellular induction of filamentation (Fig. 1e). This result suggested that an unknown factor, rather than the α pheromone, intercellularly induces unisexual mating. Intriguingly, the production of this unknown signal correlated with cell density, and the filamentous mini-colony population achieved ~100% when the cells grew at a high cell density on mating-inducing medium (Fig. 1f).

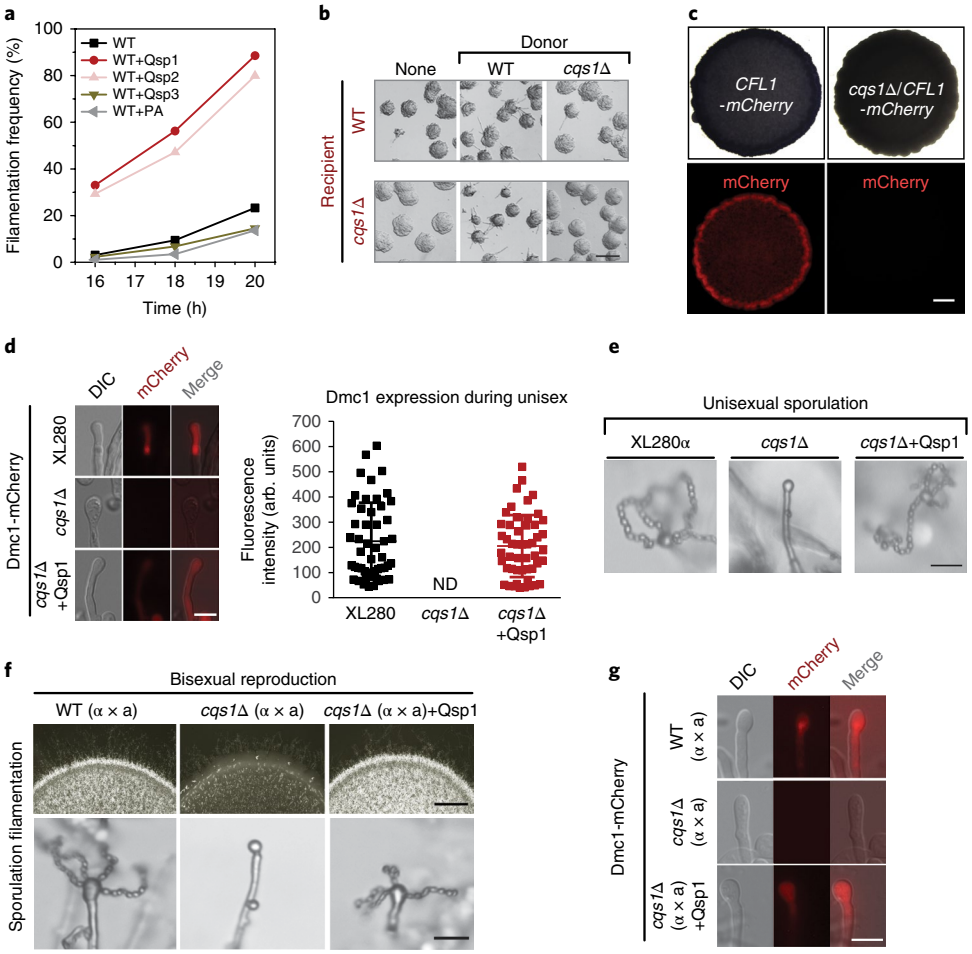

Fig. 2 | Quorum sensing peptide encoding gene *CQS1* is important for both bisexual and unisexual development. a, Effect of previously reported *Cryptococcus* quorum sensing signals on activation of filamentation during unisexual reproduction. Signals of 50 μM were used in the test. PA, pantothenic acid. Data shown are from two independent experiments. **b**, Paracrine induction of unisexual initiation needs the peptide signals encoded by *CQS1*. Scale bar, 100 μm. Representative images of $n = 5$ experiments. **c**, *CQS1* is important for expression of filamentation-specific marker protein Cfl1. Scale bar, 1 mm. Images are representative of three independent experiments conducted with similar results. **d**, Deletion of *CQS1* resulted in the defective expression of Dmc1-mCherry in basidia during unisexual mating which can be restored by supplementation of synthetic Qsp1 (final concentration, 50 μM) into the medium. The images of the fluorescence-labelled strains were taken at 7 days post mating stimulation. For each strain, 50 basidia were examined for the expression of Dmc1-mCherry. ND, undetected. Data are mean ± s.d. Scale bar, 10 μm. **e**, Disruption of *CQS1* blocked sporulation during unisexual mating. The *cqs1*Δ mutant sporulated in the presence of synthesized Qsp1. Scale bar, 20 μm. **f**, Cross between XL280α and XL280**a** led to profuse filamentation and robust sporulation. Deletion of *CQS1* substantially attenuated filamentation and abolished sporulation during bisex. These defects were restored by the addition of synthesized Qsp1. Scale bars, 1 mm (top panel), 20 μm (bottom panel). **g**, The addition of Qsp1 restored the defective expression of Dmc1-mCherry in *cqs1* × *cqs1* mutant cross. The fluorescence-labelled isogenic α and **a** strains were premixed and the mixture was subsequently plotted on V8 medium to stimulate mating. The images were taken at 7 days post mating stimulation. DIC, differential interference contrast. Scale bar, 10 μm. In **e**–**g**, images are representative of more than five independent experiments conducted with similar results.

This prompted us to test whether the unknown factor inducing the unisex is a quorum sensing molecule due to its common role in sensing population density[20]. We thus assessed the previously reported *Cryptococcus* quorum sensing signals (pantothenic acid and the quorum sensing peptides, including Qsp1, Qsp2 and Qsp3)[21,22] for their activities to stimulate self-filamentation. Among these signals, only Qsp1 and Qsp2 exerted striking induction activity (Fig. 2a). A previous study has indicated that Qsp1 and Qsp2 can rescue the cell density-associated growth defect in a serotype D *tup1*Δ strain[21], which fails to grow at low cell density. A more recent investigation has shown that Qsp1 plays an important role in mediating *Cryptococcus* virulence[23]. However, the functional role of quorum sensing peptides in sexual reproduction, considered to play an important role in promoting *Cryptococcus* infections, remains unknown[2,4].

***CQS1* is important for activation and coordination of both bisexual and unisexual development.** Peptides Qsp1, Qsp2 and Qsp3 are different isoforms, maturated from three alternatively spliced transcripts from the gene, *CQS1*[21] (Supplementary Fig. 1a). Disruption of *CQS1* substantially inhibited initiation of unisexual filaments (Figs. 1f and 2b). After extended incubation, only sparse unisexual filaments (mostly invasive hyphae) were observed in the *cqs1*Δ mutant (Fig. 1b). Furthermore, expression of the filamentation marker Cfl1 was greatly attenuated in the *cqs1*Δ mutant (Fig. 2c). The defects of filamentation and Cfl1 expression in the *cqs1*Δ mutant were rescued by synthesized Qsp1 and Qsp2, but not by Qsp3 (Supplementary Fig. 1b–c). This suggests that quorum sensing peptides represent the important paracrine signals for unisexual activation. Consistently, confrontation assays indicated that the *cqs1*Δ mutant failed to efficiently stimulate self-filamentation in

the adjacent wild-type XL280α strain (Fig. 2b). In detailed phenotypic analysis, we showed that deletion of *CQS1* had little or no effect on the formation of unfused clamp cells and monokaryotic growth (the hallmarks of unisexual hyphae) during self-filamentation, but resulted in remarkably shorter filaments compared with the wild-type strain (Supplementary Fig. 2a–c). These data suggest that *CQS1* affects both hyphal initiation and extension during unisexual development.

To examine whether quorum sensing peptide as the important signalling molecule controls unisexual meiotic reproduction or is merely involved in hyphal differentiation as a morphogen, we investigated its functional role in meiotic cycle, which is the hallmark of sex. Early studies have identified meiosis-specific recombinase Dmc1, whose expression is essential for meiotic progression and the formation of four meiotic spore chains in *C. neoformans*[24,25]. Deletion of *CQS1* resulted in the undetectable expression of mCherry-fused Dmc1 in basidia and completely blocked meiotic sporulation, even after prolonged incubation (Fig. 2d–e). Again, these defects can be compensated by synthesized Qsp1 (Fig. 2d–e).

To test whether *CQS1*-activated unisex is unique to the XL280α background, *CQS1* was mutated in the JEC21α background, which can undergo haploid fruiting but less abundantly than XL280α[17]. The JEC21α-derived *cqs1*Δ mutant failed to filament, even after 1-month incubation (Supplementary Fig. 3). Likewise, such failure was suppressed by synthesized Qsp1. Furthermore, we performed a bilateral mating assay to determine whether *CQS1* is also important for bisexual reproduction. We showed that bisexual filamentation was substantially decreased in bilateral mating (α *cqs1*Δ × **a** *cqs1*Δ), in which neither sporulation nor the expression of Dmc1-mCherry was observed (Fig. 2f–g). As expected, these bisexual defects were restored by the synthesized Qsp1 (Fig. 2f–g). We further investigated the regulatory relationship between Qsp1 and the α mating pheromone in two sexual forms using quantitative PCR with reverse transcription (qRT–PCR) analysis. We found that deletion of *CQS1* reduced the messenger RNA levels of Mfα-coding genes during both bisexual and unisexual mating, but not vice versa (Supplementary Fig. 4). Considering the critical role of Mfα in bisexual activation[15], Qsp1 activates bisexual mating at least partially via its control of the α pheromone.

Qsp1 stimulates mating response through the control of Mat2. To reveal the *Cryptococcus* genes controlled by *CQS1*, we performed transcriptomic analysis via high-coverage RNA sequencing (RNA-seq). One hundred and nine genes were found to be differentially expressed in *cqs1*Δ compared with the wild-type strain during unisexual development (Fig. 3a and Supplementary Table 1). Among these, 103 genes were also differentially expressed in the *cqs1*Δ mutant grown in the presence of synthetic Qsp1 or Qsp2 compared with the *cqs1*Δ mutant grown in the absence of the synthetic peptides (Fig. 3a and Supplementary Table 1). Importantly, the regulons of Qsp1 and Qsp2, but not Qsp3, were enriched with genes involved in different processes associated with mating (Fig. 3b–c). This echoes the aforementioned observation that Qsp3 failed to stimulate unisex in the *cqs1*Δ mutant (Supplementary Fig. 1b). On the basis of RNA-seq data, we identified only the transcript isoform encoding the Qsp1 precursor and no other *CQS1* transcript isoform for other peptides (Supplementary Fig. 5). This indicates the exclusive role of Qsp1 among *CQS1*-derived quorum sensing peptides during unisexual reproduction.

Among Qsp1-regulated genes, ~64% exhibited differential expression after transferring cells cultured under mating-repressing condition onto mating-inducing medium, and are referred to as mating-responsive genes. This percentage was much higher than the ratio of mating-responsive genes in the *Cryptococcus* genome (Fig. 3d). To further define the genes responsible for Qsp1-mediated mating response, the expression profiles of the *cqs1*Δ mutant responding to synthetic Qsp1 in different amounts (4, 16 and 512 nM) were compared, and three sets of genes were grouped based on the sensitivity of their transcriptional response to Qsp1, as revealed by RNA-seq analysis (Fig. 3e). Among these gene sets, we concentrated on the group of genes (group I) that showed transcriptional response to 4 nM Qsp1 in the *cqs1*Δ mutant. This concentration was chosen because it successfully induced unisexual filamentation in the *cqs1*Δ mutant at a level comparable to the wild-type strain (Supplementary Fig. 6). We systematically assessed the expression patterns of the genes belonging to group I according to their differential expression in response to different amounts of Qsp1 or Qsp3 (as a negative control) in the *cqs1*Δ mutant. The major expression pattern, which covered ~29% of the group I genes (Fig. 3f, top panel), greatly resembled that of the mating MAPK pathway members (Fig. 3f, bottom panel). Thus, the genes belonging to this group probably contain the major Qsp1 regulon members responsible for the induction of the mating response. Due to the generally crucial role of DNA-binding transcriptional factors in mastering biological processes, we specifically focused on the six transcriptional factors present in group I (Fig. 3g and Supplementary Fig. 7a–c). These regulators were individually overexpressed in the *cqs1*Δ mutant and the resultant strains were tested for the capability to induce unisexual filamentation. We found that overexpression of two previously known regulators, Mat2 and Znf2, restored the defect of self-filamentation in the absence of *CQS1* (Fig. 3g). Znf2 is a known master regulator of filamentation that functions downstream of Mat2 during unisexual mating[12,26]. Therefore, Qsp1 probably upregulates Mat2, which activates Znf2 to execute morphogenesis. Indeed, we found that Qsp1 upregulated the expression of *MAT2* during unisexual mating (Fig. 3h) and there was a marked overlap between Qsp1 and Mat2 targets (Fig. 3i).

Many quorum sensing factors guide microbial behaviours by sensing external stimulation[27]. The transcriptomic data indicated that Qsp1 influenced the expression of a set of genes potentially responsible for glucose response (Fig. 3c). In some fungi, glucose as a key metabolic/nutritional signal modulates sexual development[28]. This promoted us to test whether glucose affects sexual differentiation and mating response in *C. neoformans*. We found that glucose strongly inhibited self-filamentation and invasive growth, a cell–substrate adhesion process coupled with filamentous differentiation in *C. neoformans*[26] (Fig. 4a–c). In contrast, these morphological behaviours were readily observed in the presence of alternative carbon sources, such as galactose, but were completely eliminated in cells where *CQS1* is absent (Fig. 4a–c).

We further used RNA-seq analysis to evaluate the effect of different carbon sources on the induction of mating MAPK genes in the presence or absence of Qsp1 (Fig. 4d and Supplementary Table 2). We found that multiple components of the mating MAPK signalling cascade were highly induced at 12 h after incubation of XL280α cells on the plate containing galactose as the sole carbon source, but the induction was greatly attenuated in the absence of Qsp1. In contrast, when using glucose as the carbon source, no evident induction in the expression of mating MAPK pathway members was observed, regardless of the presence of Qsp1. Together, these results suggest that starvation for glucose stimulates the mating response in a Qsp1-dependent manner.

Atypical zinc finger regulator Cqs2 is an important component of Qsp1 signalling during both bisexual and unisexual reproduction. To identify the important components of the Qsp1 signalling pathway, we developed a multi-layered genetic screening method based on random insertional mutagenesis via *Agrobacterium*-mediated transformation (Fig. 5a). We generated ~42,000 insertional mutants in the XL280α parental strain and screened for a combination of phenotypes, including the defect in self-filamentation and an inability to respond to synthetic Qsp1. The genomic DNA of

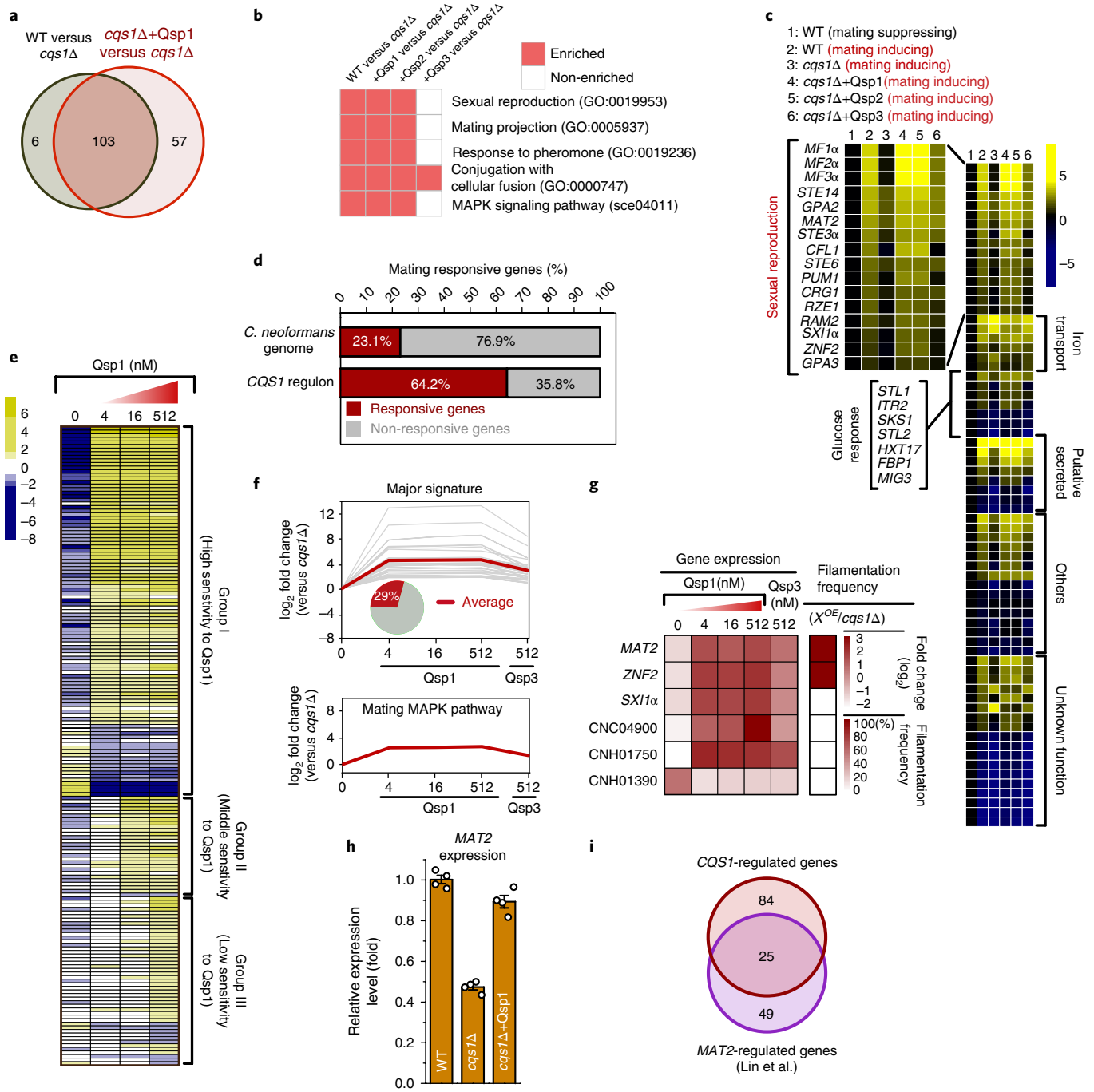

Fig. 3 | Qsp1 mediates mating response through the control of Mat2. a, Venn diagram analysis indicates that *CQS1* regulates gene expression largely through the paracrine control exerted by its peptide product. The strains were cultured on V8 (pH = 7) agar with or without synthetic Qsp1 peptide (512 nM). **b**, Identification of gene ontology terms associated with fungal mating among DEGs of the *cqs1*Δ mutant in the presence of different quorum sensing peptides (512 nM each). Gene ontology analysis was performed using the DAVID gene ontology program. GO, gene ontology. **c**, Gene expression of *C. neoformans* cells under different conditions. Colour bar represents $\log_2$ relative expression values versus column 1. **d**, *CQS1* controls many mating-responsive genes. **e**, Transcriptional profiling of the *cqs1*Δ mutant responding to different amounts of synthetic Qsp1 (4, 16 and 512 nM). Colour bar indicates $\log_2$ fold change values. Column '0' represents the *cqs1*Δ mutant without peptide treatment. **f**, Expression patterns of genes belonging to group I based on their differential expression pattern in response to Qsp1 with different amounts (4, 16 and 512 nM) and Qsp3 (512 nM) in the *cqs1*Δ mutant. Top and bottom panels indicate the major expression pattern of genes in group I and the expression pattern of mating MAPK pathway genes, respectively. The average expression level across all genes with the major pattern is shown with a red line. **g**, Overexpression of Mat2 and Znf2 can rescue the defect of filamentation in the *cqs1*Δ mutant. Left panel: gene expression of group I regulators under different conditions ($n = 2$ independent RNA-seq experiments). Right panel: filamentation frequency when group I regulators were overexpressed in *cqs1*Δ mutant ($n = 4$ independent experiments). 'X' indicates regulatory gene controlled by Qsp1. **h**, Qsp1 positively regulates the expression of *MAT2*. Data are mean ± s.e.m. of four independent experiments. **i**, Comparison of *CQS1*-regulated and *MAT2*-controlled genes under mating-inducing condition. Original transcriptome data of *mat2*Δ were obtained from a previous study[12]. In **a**–**f** and **i**, all RNA-seq data are from two independent experiments.

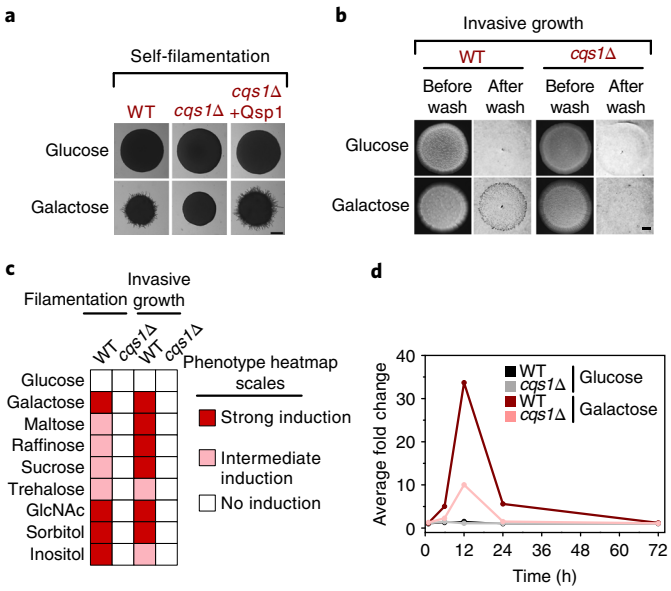

Fig. 4 | Qsp1 participates in glucose starvation-induced mating response and morphogenesis. a,**b**, Carbon source-dependent filamentation (**a**) and invasive growth (**b**). Strains were grown on YP agar containing different carbon sources for 3 days (representative images of $n = 5$ experiments). For invasive growth, the plates were washed with cold water, and the remaining invasive cells embedded in agar were photographed. Scale bars, 100 μm (**a**), 1 mm (**b**). **c**, Phenotype scores are represented in distinct colours based on semiquantitative analysis targeting the phenotypes related to different carbon sources. Results represent at least three independent experiments. **d**, Fold induction of MAPK pathway genes during the incubation on the media containing different carbon sources in the presence or absence of Qsp1. *Cryptococcus* cells cultured under extremely mating-repressing conditions (YPD liquid condition) were transferred onto solid plates containing glucose or non-favoured sugar galactose as the sole carbon source for inducing mating response. Data shown are from two independent experiments.

mutants meeting all criteria were extracted, pooled and subjected to *Agrobacterium*-mediated insertional mutagenesis sequencing (AIM-seq) to identify the insertion sites[29]. Multiple independent genetic loci were identified (Supplementary Table 3), including *OPT1*, which encodes an oligopeptide transporter[23]. Most recently, Homer et al. have shown that in the serotype A cryptococcal strain H99, Opt1 as a critical member of Qsp1 cascade is responsible for the internalization of secreted Qsp1[23]. We found that the phenotypes associated with the *opt1*Δ mutant in XL280α bore a striking resemblance to those observed in the *cqs1*Δ mutant, including the defect of unisexual activation and Cfl1 expression (Supplementary Fig. 8a–b). However, these defects cannot be restored by synthesized Qsp1, suggesting that the internalization of Qsp1 by Opt1 is probably a central mechanism essential for different processes mediated by Qsp1. Moreover, RNA-seq analysis revealed a great overlap between Opt1-regulated genes and Qsp1 targets (Supplementary Fig. 8c and Supplementary Table 4). The identification of *OPT1* also points to the efficacy and specificity for our screening strategy. Besides, we explored an insertion in proximity to the start site of CNF00370 (designated as *CQS2*) transcript using AIM-seq in combination with high-coverage RNA-seq analysis (Fig. 5b). We further confirmed that *CQS2* serves as an important component of Qsp1 signalling pathway during both bisex and unisex, on the basis of the following findings: (1) its mRNA level was upregulated by Qsp1 (Fig. 5b); (2) *CQS2* deletion greatly impaired bisexual and unisexual filamentation, considerably decreased expression of Cfl1 during self-filamentation and abolished meiotic sporulation during both bisex and unisex (Fig. 5c–f); (3) synthetic Qsp1 cannot complement these defects in the *cqs2*Δ mutant (Fig. 5c–f); (4) transcriptomically, ~42.9% targets of Cqs2 were also regulated by Qsp1 (Fig. 5g and Supplementary Table 5) and none of the targets of Cqs2 showed significant transcriptional response to Qsp1 in the *cqs2*Δ mutant during unisex (Fig. 5h). Together, these data suggest that Cqs2 is an important component of Qsp1 signalling pathway that promotes bisex and unisex.

Cqs2 protein does not possess any apparent domain except for a predicted nuclear localization signal (Fig. 6a). This is consistent with our observation that Cqs2-mCherry was enriched in the nucleus during unisexual mating (Fig. 6b). Upon further analysis in combining a Position-Specific Iterative BLAST analysis with Rosetta ab initio and comparative modelling methodology[30], we identified a C2H2 zinc finger motif harboured in a 65-residue region that is highly conserved among proteins from phylogenetically divergent fungi (Fig. 6a,c and Supplementary Fig. 9). The C2H2 zinc fingers are the best-characterized class of zinc fingers to date and are extremely common in fungal transcription factors[31]. However, this conserved region of Cqs2 contains only one finger, and all characterized fungal C2H2 domains contain more than two. To examine the functional role of this 'atypical' zinc finger motif in the unisexual induction activity of Cqs2, two cysteine residues predicted to be critical for zinc ion binding in the zinc finger motif were substituted with alanine to generate mutated $Cqs2^{C416A/C421A}$. We found that mCherry-tagged $Cqs2^{C416A/C421A}$ localized normally and was expressed abundantly in cultured cells (Fig. 6b). However, forced expression of this mutated protein did not stimulate unisex in the *cqs2*Δ mutant, in which self-filamentation was substantially promoted as the wild-type version of Cqs2 was overexpressed (Fig. 6d).

To determine the capability of 'atypical' C2H2 zinc finger protein Cqs2 to associate with DNA in vivo, we used chromatin immunoprecipitation (ChIP) assay to test whether it associates with its own promoter because many C2H2 members display auto-regulatory activities[32]. ChIP analysis was performed using anti-mCherry antibody (ChIP grade), and quantitative PCR (qPCR) was used to evaluate the occupancy of Cqs2-mCherry at different locations upstream of or within the open reading frame (ORF) of *CQS2*. We identified an evident enrichment of Cqs2-mCherry protein at the region surrounding the start site of the transcript of *CQS2* identified by RNA-seq assay (Figs. 5b and 6e). The enrichment was significantly reduced in cells expressing $Cqs2^{C416A/C421A}$-mCherry (Fig. 6e). These results indicate that Cqs2 associates with DNA, and specifically with its own promoter, and the zinc finger motif is important for its DNA association.

Discussion

In fungi, mating pheromone represents the best studied paracrine signal for sexual activation and it induces mating response through specific recognition by Ste2 or Ste3 type G protein-coupled receptors (GPCRs) upon external stimulation[33,34]. *Cryptococcus MAT*α cells harbour two Ste3 type GPCR genes: *STE3*α[14] and *CPR2*[35]. *STE3*α appears not to affect haploid fruiting[14]. By comparison, the expression of Cpr2 is important to induce unisex, but its activity for unisexual activation is constitutive and independent of ligands[35]. This evidence indicates that both GPCRs are unlikely to be involved in the direct recognition of secreted Mfα during unisexual mating, supporting the notion that the inability of Mfα to efficiently stimulate unisex in *C. neoformans* may be attributed to the lack of compatible GPCR receptor for its perception. We propose that such inability of the pheromone paracrine system may reflect the uniqueness of the unisexual cycle. Most eukaryotes, including *Cryptococcus*, engage in bisexual mating, in which nuclear fusion after cell–cell fusion (syngamy) between two compatible mating partners is the major

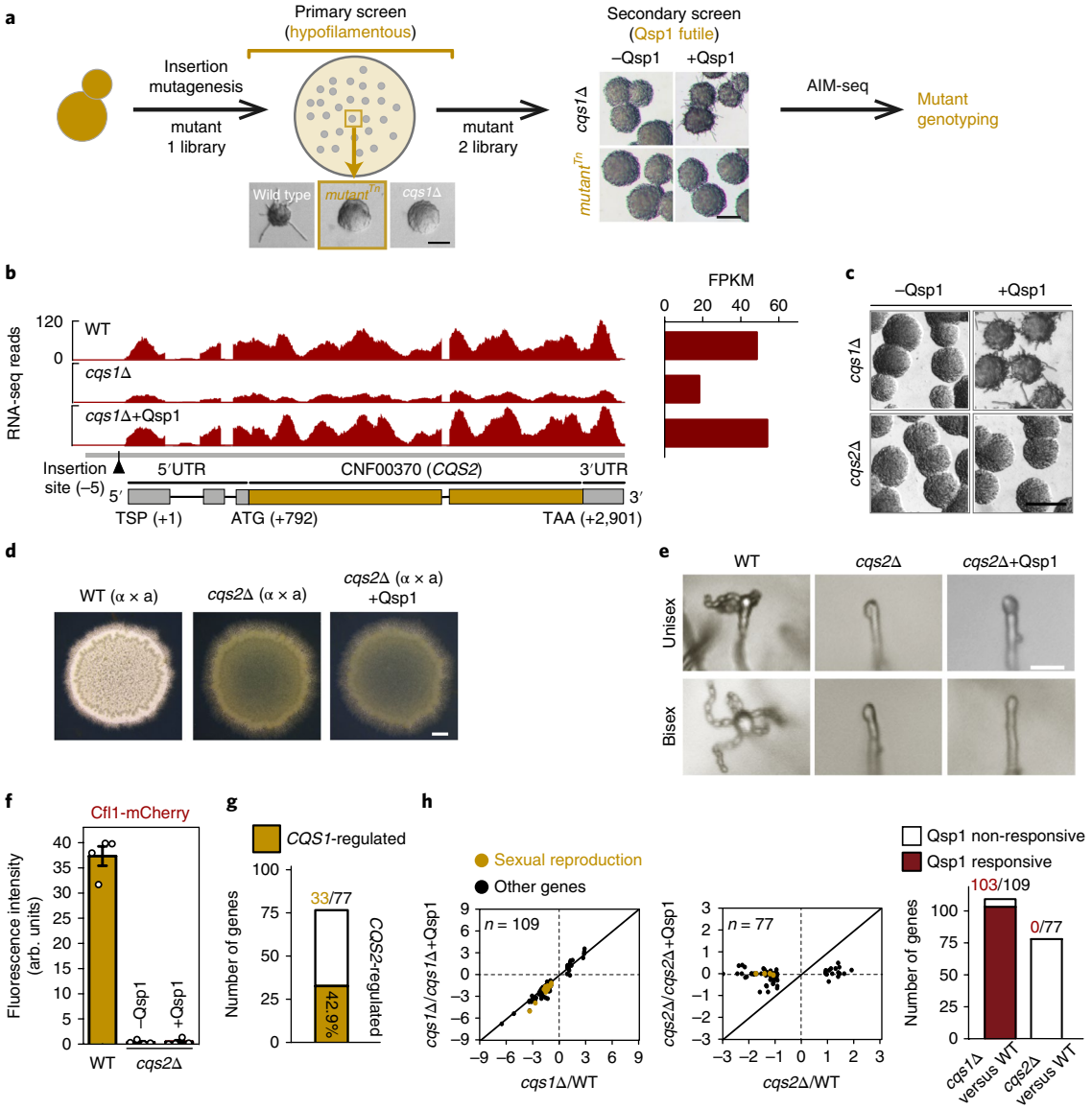

Fig. 5 | Cqs2 as an important Qsp1 signalling cascade member promotes bisexual and unisexual mating. a, A schematic diagram depicting the multi-layered genetic screening method developed to identify Qsp1 signalling genes. Mutant 1 library, the mutants generated via insertional mutagenesis; mutant 2 library, the hypofilamentous mutants identified based on self-filamentation assay. Scale bar, 100 μm. **b**, Diagram of the *CQS2* (CNF00370) locus in the XL280α background based on RNA sequence reads. The arrow indicates the location of the insertion site in the *CQS2*^{Tn} mutant. TSP indicates the transcriptional start point of *CQS2*. Enriched RNA-seq signals visualized by Integrated Genome Browser are representative of two independent experiments. FPKM, fragments per kilobase of exon per million fragments mapped; UTR, untranslated region. **c**, Rescue effect of synthetic Qsp1 on the defects of unisexual filamentation in *cqs2*Δ mutant. Scale bar, 100 μm. **d**, Bisexual filamentation for a wild-type cross between XL280α and XL280a and *cqs2*Δ bilateral mutant crosses. All mating patches were spotted on V8 medium with or without synthetic Qsp1 (final concentration, 50 μM). Scale bar, 1 mm. **e**, *CQS2* is essential for bisexual and unisexual sporulation. Bisexual sporulation was assessed in wild-type (XL280α × XL280**a**), and bilateral (α *cqs2*Δ × **a** *cqs2*Δ) mating assays on V8 medium with or without synthetic Qsp1 for 7 days. For unisexual sporulation, the wild-type strain XL280α and the *cqs2*Δ mutant were incubated on V8 medium in the presence or absence of Qsp1 for 7 days post inoculation. Scale bar, 20 μm. **f**, Deletion of *CQS2* attenuated the expression of Cfl1-mCherry and synthetic Qsp1 cannot rescue this defect. Data are mean ± s.e.m. of four independent experiments. **g**, Overlap of Cqs2-regulated genes with Qsp1-regulated genes ($n = 2$ independent experiments). **h**, No Cqs2 targets showed differential expression in response to Qsp1 in the *cqs2*Δ mutant ($n = 2$ independent experiments). In **c**–**e**, images are representative of more than five independent experiments conducted with similar results.

mechanism involved in ploidy duplication before meiotic progression[36]. Previous research has indicated that unisex in *C. neoformans* can occur independently of syngamy[8,26,37]. Instead, endo-replication or cell fusion-independent karyogamy processes have been proposed as an alternative route to elevate ploidy[8]. Given that sexual syngamy is generally attributed to the control by pheromone in fungi[38], unisex-specific syngamy-independent diploidization may provide a plausible explanation regarding why the intercellular regulation mediated by pheromone is not strictly required for unisexual reproduction in *C. neoformans*.

We show that the paracrine regulation exerted by quorum sensing molecule Qsp1 is important for both bisexual and unisexual reproduction in *C. neoformans*. Notably, cell density-dependent regulation of sexual reproduction, which is potentially medi-

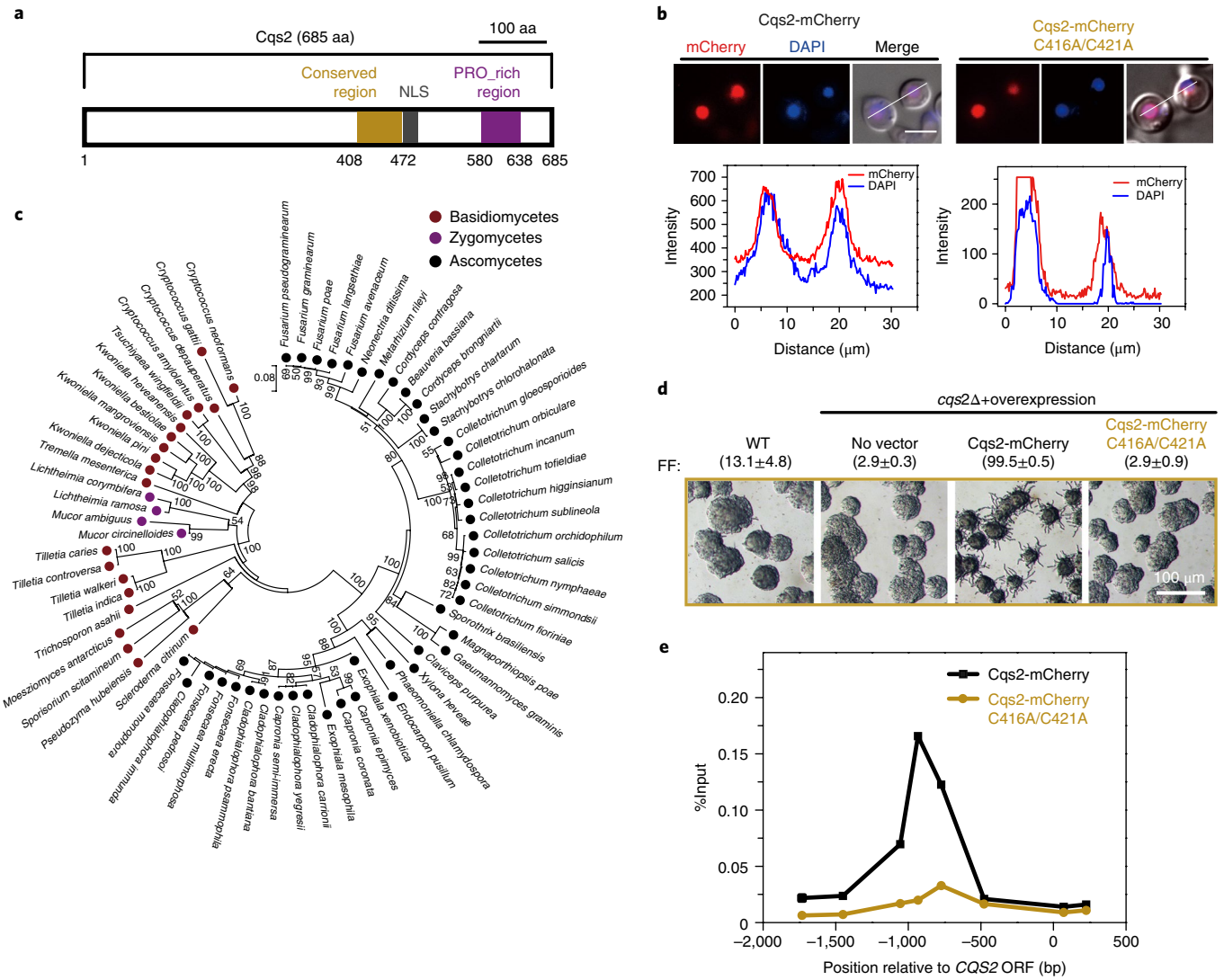

Fig. 6 | Cqs2 can associate with its own promoter through an atypical C2H2 zinc finger domain conserved among divergent fungal species. a, Domain organization of Cqs2. NLS, nuclear localization signal. **b**, Localization of Cqs2-mCherry and Cqs2$^{C416A/C421A}$ -mCherry (>120 cells for each were examined) during unisexual reproduction (top), and fluorescence intensity plot along a cellular axis indicated with a white line on the merged image (bottom). DAPI, 4′,6-diamidino-2-phenylindole. Scale bar, 5 μm. **c**, Phylogenetic tree of Cqs2 homologues. Protein sequences were aligned using neighbour-joining method with the MEGA v.5.04 program. **d**, The *CQS2*$^{C416A/C421A}$ mutant allele cannot restore the defect of filamentation in the *cqs2*Δ mutant. Filamentation frequency was calculated based on the percentage of filamentous mini-colonies 21 h after mating induction. Data are presented as the mean ± s.d. from four independent experiments. FF, filamentation frequency. **e**, Chromatin immunoprecipitation (ChIP) was performed with anti-mCherry antibody in *cqs1*Δ mutant cells, in which the mCherry-fused Cqs2 or Cqs2 $^{C416A/C421A}$ were overexpressed. ChIP enrichment was detected by qPCR across an approximately 2-kb region upstream of or within the *CQS2* ORF. Data shown are from two independent experiments.

ated by a quorum sensing-like molecule, has also been observed in other fungal species[39,40]. For instance, in *Candida albicans*, the mating efficiency has been found to be positively linked with inoculum size when cells are grown anaerobically[40]. Because the Qsp1 system is not present in *C. albicans*, the effect of cell density-dependent control on sexual regulation may have arisen via convergent evolution. In bacteria, the quorum sensing system commonly coordinates gene expression in response to nutritional or environmental stressors. Early studies implicated that quorum sensing may have the same function in some fungi. For instance, in budding yeast, quorum sensing molecules phenylethanol and tryptophol have been found to control morphogenesis under nitrogen starvation conditions[41]. We also demonstrate that Qsp1 can stimulate mating response in response to glucose starvation, an important nutritional signal for many fungi. Nutritional and environmental stress has been broadly demonstrated in fungi to be involved in sexual initiation[42,43]. In this regard, the quorum sensing system may play a general role as an intercellular circuit in bridging sexual control and perception of surrounding stress in fungi or other eukaryotic microbes.

Methods

Strains, culture conditions, mating and phenotypic assays. Strains used in this study are listed in Supplementary Table 6. All mutant strains were generated in the reference strains XL280α, a model *C. neoformans* strain used to investigate unisexual reproduction[17], or JEC21α, which can undergo unisex, but less robustly than the former. *Cryptococcus* strains were cultured on YPD solid plates (20 g per l glucose, 20 g per l peptone, 10 g per l yeast extract, 2% agar) at 30°C for routine growth and V8 agar (5% v/v V8 juice, 0.5 g per l KH_2PO_4, 4% agar) for mating assays, unless otherwise indicated. For bilateral mating assays, a and α cells in equal numbers (original absorbance $A_{600\ nm} = 1.0$) were premixed and cocultured on V8 juice agar in the dark at 25 °C. For quantitative analysis of filamentation frequency,

cells of strains were plated onto V8 medium at a low cell density and allowed to grow into isolated mini-colonies after 1 day of culture. Mini-colonies exhibited a remarkable heterogeneity in filamentation, and the filamentous incidence among mini-colonies reflects the strength of unisexual induction. For carbon source-induced morphogenesis assays, YP medium (20 g per l peptone, 10 g per l yeast extract, 2% agar) without glucose was used as the base medium, to which a given carbon source was added to a final concentration of 2% (w/v). Strains carrying genes driven by the inducible promoter of the *CTR4* gene were grown in medium supplemented with 25 μM $CuSO_4$ for suppression or 200 μM bathocuproine disulphonate for induction. Self-filamentation and sporulation were examined microscopically as previously described[25]. Since Qsp1 is highly diffusible, plates were cut to separate the *cqs1*Δ mutant from other strains harbouring the intact *CQS1* gene before the examination of phenotypes, unless otherwise indicated. All peptides used for mating and phenotypic assays were synthesized by Shanghai Qiangyao Bio-technology Co. Ltd.

Gene knockout and overexpression. For gene disruption, overlap PCR products were generated with NEO (Neomycin)/NAT (Nourseothricin) resistance cassette and 5′ and 3′ flanking sequences (1.2–1.5 kb) of the coding genes from strain XL280α as previously described[26]. The PCR product was directly introduced into strain XL280α by biolistic transformation. The resultant mutants were confirmed by PCR and genetic crosses. For gene overexpression, genes (ORF) were amplified by PCR and the amplified fragments were digested with proper restrictive digestion enzymes and inserted into pXC after the *CTR4* promoter as previously described[26]. Overexpression plasmids were linearized via restriction enzyme digestion before being introduced into relevant *Cryptococcus* strains through biolistic transformation or electroporation as we previously described[12]. Primers for gene disruption and overexpression used in this study are listed in Supplementary Table 7.

Microscopy and fluorescence. To examine the subcellular localization of Cqs2 during unisexual reproduction, strains harbouring P_{CTR4}-*CQS2-mCherry* were grown on V8 agar containing bathocuproine disulphonate at 25 °C for 48 h. 4,6-diamidino-2-phenylindole (5 mg per ml) was used for nucleus staining before microscopic examination. To investigate the effect of *CQS1* on the expression of Dmc1, cells from different strains harbouring P_{DMC1}-*DMC1-mCherry* were dropped on V8 agar plates and incubated at 25 °C for 7 days. Images were acquired and processed with a Zeiss Axioplan 2 imaging system with the AxioCam MRm camera software Zen 2011 (Carl Zeiss Microscopy).

Confrontation analysis. The confrontation assay was used to test whether secreted factors from the wild-type strain can induce unisexual mating in *Cryptococcus* strains. The donor strain cell suspension (3 μl ($A_{600\,nm}$ = 3.0)) was dropped onto a V8 plate and incubated in the dark for about 72 h at 25 °C for the accumulation of the paracrine signal. Then, 3 μl low cell density recipient cells ($A_{600\,nm}$ = 0.05–0.1) were dropped in close proximity to the donor strain. Filamentation frequency was calculated based on the percentage of filamentous mini-colonies of the recipient strain.

Site-directed mutagenesis. We introduced single nucleotide mutations into *CQS2* coding region to generate the mutant allele encoding $Cqs2^{C416A/421A}$ using the QuikChange II XL site-directed mutagenesis kit (Agilent Technologies). Primers for mutagenesis (Supplementary Table 7) were designed using the QuikChange primer design program (Agilent Technologies).

RNA purification and RT–PCR analyses. Frozen pellets were ground in liquid nitrogen and total RNA was purified using the Ultrapure RNA Kit (Kangweishiji, CW0581S) according to the manufacturer's instructions, and then reverse-transcribed with the Fastquant RT Kit (Tiangen KR106-02, with gDNase). Relative expression level of selected genes was measured by real-time RT–PCR using power SYBR qPCR premix reagents (KAPA) in a CFX96 Touch Real-Time PCR Detection System (Biorad). Primers for qPCR used in this study are listed in Supplementary Table 7. Relative transcript levels were calculated to fold change and normalized to the *TEF1* gene using the comparative C_t (threshold cycle) method as previously described[26].

RNA-seq and data analysis. For RNA-seq analysis evaluating the impact of Qsp1 signalling components on mating response, the wild-type XL280α strain and isogenic Qsp1 pathway mutants were cultured in YPD liquid medium (extremely mating-inhibitory condition) at 30 °C overnight. The overnight cell culture was then washed by cold water, and plotted on V8 agar (pH = 7) with or without synthetic peptide or YP plates containing different carbon sources for mating induction. Cells were collected at 12 h post mating stimulation for isolation of total RNA, unless otherwise indicated. RNA levels and integrity were determined by Qubit RNA Assay Kit in Qubit 2.0 Flurometer (Life Technologies, CA, USA) and RNA Nano 6000 Assay Kit of the Bioanalyzer 2100 system (Agilent Technologeis, CA, USA), respectively. RNA purity was evaluated using the Nano Photometer spectrophotometer (IMPLEN, CA, USA). Illumina complementary DNA libraries were generated using VAHTS mRNA-seq v2 Library Prep Kit (Vazyme Biotech Co., Ltd, Nanjing, China) according to the manufacturer's instructions. RNA deep sequencing was performed by Annoroad Gene Technology Co., Ltd (Beijing, China). Samples were clustered using VAHRS RNA adapters set1/set2 and sequenced using Illunima Hiseq 4000 platform in a 2 × 150 pair-ended manner.

Initial quality control of the sequencing data was performed using FastQC v0.11.5 software. After initial quality control, Hisat v0.1.6-beta was used for clean short reads (~2 GB clean data for each sample, representing over 100 × coverage of the total transcriptome) mapping to the annotated genome sequence of *C. neoformans* JEC21. The gene expression level was measured in fragments per kilobase of exon per million fragments mapped by Stringtie v1.2.1. The differential expression of genes (DEGs) was assessed using the Gfold v1.1.2 program[44]. Twenty-seven DEGs were chosen for quantitative real-time PCR to confirm the reproducibility of the RNA-seq results. The genes with significant differential expression or significant transcriptional response to synthesized Qsp1 (Fig. 3e) were defined on the basis of the fold change criterion ($|\log_2(\text{fold change})| > 0.9$). This criterion was determined according to gene functional grouping analysis, which enables precise assessment of biological significance of a given fold change. DAVID gene ontology program (https://david.ncifcrf.gov/) was performed for gene ontology analysis. The heat maps were generated using the pheatmap package in R version 3.4.2.

***Agrobacterium tumefaciens*-mediated random insertional mutagenesis and AIM-seq.** Random insertion mutagenesis was carried out as previously described using *A. tumefaciens* strain EHA105 carrying the PZP-NEO/NATcc plasmid with small modifications. Briefly, *A. tumefaciens* was incubated overnight with shaking at 28 °C in Luria–Bertani broth containing kanamycin. Then the overnight *A. tumefaciens* cells were washed and resuspended at an $A_{660\,nm}$ of 0.15 in liquid induction medium with 200 μM acetosyringone, shaking at 22 °C for 6 h, or until the final concentration reached an $A_{660\,nm}$ of 0.6. An overnight culture of *C. neoformans* XL280α was collected and diluted in induction medium to a final concentration of 10^6–10^7 cells per ml. Equal volumes (200 μl) of *A. tumefaciens* and *C. neoformans* cells were then mixed, dropped without spreading on induction medium agar (with acetosyringone) and co-incubated at 22 °C for 2–3 days before being scraped onto selection media (YPD + 100 μg per ml nourseothricin + 100 μg per ml cefotaxime). Colonies were then transferred into YPD liquid media and incubated at 30 °C for 2–3 days before freezing down and/or screening.

For AIM-seq, the genomic DNA of the AIM mutants identified were pooled together with equal concentration to a final amount of 14.4 μg before whole genome sequencing using Illumina Hiseq 4000 (2 × 150-bp pair-ended reads). The resulting sequence data contained 1.2×10^6 read pairs (~10 × genomic coverage per strain). The AIM-seq analysis was performed online at https://github.com/granek/aimhii. A reference genome sequence, DNA sequence inserted, adapter sequences and reads data sequenced in FASTQ format (either single-end or paired-end) are needed for AIM-HII analysis. The appropriate adapter sequence was supplied by Illumina. AIM-HII pairs the clusters that are within the specified gap limit and flank opposite ends of the insert into 'cluster pairs'. We refer to those unpaired clusters which have no partner identified as 'singleton clusters'.

Chromatin immunoprecipitation. ChIP assays were performed as described previously with modifications[45]. In brief, cells incubated on V8 plates were harvested at 8 h post inoculation, and were cross-linked with 1% formaldehyde for 15 min. The cross-link was subsequently quenched with glycine at a final concentration of 125 mM for 5 min. Chromatin fragmentation was achieved by micrococcal nuclease (New England BioLabs) digestion for 15 min at 37 °C. Two units of micrococcal nucleases were used for samples per milligram total protein contained. Nuclear membrane was then disrupted by sonication (Diagenode Biorupter) at 4 °C. Clarified chromatin extracts were incubated with ChIP grade anti-mCherry antibody (Chromo Tek, RFP-TRAP, rtma-20, coupled to magnetic beads) overnight with agitation. After stringent washes and elution, elutes were reverse cross-linked and de-proteinated with NaCl and protease K at 65 °C for 4 h. Then, DNA was extracted using phenol-chloroform, followed by ethanol precipitation with glycan. ChIP–qPCR assays were performed with primers at different locations upstream of or within *CQS2* ORF. The enrichment of the signal was quantified as percentage of input for each primer pair. All primers used in ChIP–qPCR analyses are shown in Supplementary Table 7.

Statistical analysis. Statistical analyses were performed with R, version 3.4.2. We used a two-tailed unpaired Student's *t*-test to compare the mean florescence intensity or transcript levels from two groups. For all analysis, $P < 0.05$ was considered significant and $P < 0.001$ was considered very significant. Data are shown as means ± s.d. or means ± s.e.m. from three or more independent experiments.

Reporting Summary. Further information on experimental design is available in the Nature Research Reporting Summary linked to this article.

Data availability. The data that support the findings of this study are available from the corresponding author upon request. The GEO accession number for the RNA-seq data reported in this study is GSE94091.

Received: 26 January 2017; Accepted: 16 April 2018;
Published online: 21 May 2018

References

1. Ene, I. V. & Bennett, R. J. The cryptic sexual strategies of human fungal pathogens. *Nat. Rev. Microbiol.* **12**, 239–251 (2014).
2. Heitman, J., Carter, D. A., Dyer, P. S. & Soll, D. R. Sexual reproduction of human fungal pathogens. *Cold Spring Harb. Perspect. Med.* **4**, a019281 (2014).
3. Dyer, P. S. & O'Gorman, C. M. Sexual development and cryptic sexuality in fungi: insights from *Aspergillus* species. *FEMS Microbiol. Rev.* **36**, 165–192 (2012).
4. Ni, M., Feretzaki, M., Sun, S., Wang, X. & Heitman, J. Sex in fungi. *Annu. Rev. Genet.* **45**, 405–430 (2011).
5. Phadke, S. S., Feretzaki, M., Clancey, S. A., Mueller, O. & Heitman, J. Unisexual reproduction of *Cryptococcus gattii*. *Plos ONE* **9**, e111089 (2014).
6. Roach, K. C., Feretzaki, M., Sun, S. & Heitman, J. Unisexual reproduction. *Adv. Genet.* **85**, 255–305 (2014).
7. Wang, L. & Lin, X. Mechanisms of unisexual mating in *Cryptococcus neoformans*. *Fungal Genet. Biol.* **48**, 651–660 (2011).
8. Fu, C. & Heitman, J. *PRM1* and *KAR5* function in cell–cell fusion and karyogamy to drive distinct bisexual and unisexual cycles in the *Cryptococcus* pathogenic species complex. *PLoS Genet.* **13**, e1007113 (2017).
9. McClelland, C. M., Chang, Y. C., Varma, A. & Kwon-Chung, K. J. Uniqueness of the mating system in *Cryptococcus neoformans*. *Trends Microbiol.* **12**, 208–212 (2004).
10. Kozubowski, L. & Heitman, J. Profiling a killer, the development of *Cryptococcus neoformans*. *FEMS Microbiol. Rev.* **36**, 78–94 (2012).
11. Davidson, R. C., Nichols, C. B., Cox, G. M., Perfect, J. R. & Heitman, J. A. MAP kinase cascade composed of cell type specific and non-specific elements controls mating and differentiation of the fungal pathogen *Cryptococcus neoformans*. *Mol. Microbiol.* **49**, 469–485 (2003).
12. Lin, X., Jackson, J. C., Feretzaki, M., Xue, C. & Heitman, J. Transcription factors Mat2 and Znf2 operate cellular circuits orchestrating opposite- and same-sex mating in *Cryptococcus neoformans*. *PLoS Genet.* **6**, e1000953 (2010).
13. Hsueh, Y. P. & Shen, W. C. A homolog of Ste6, the a-factor transporter in *Saccharomyces cerevisiae*, is required for mating but not for monokaryotic fruiting in *Cryptococcus neoformans*. *Eukaryot. Cell* **4**, 147–155 (2005).
14. Chung, S. et al. Molecular analysis of *CPR*alpha, a MATalpha-specific pheromone receptor gene of *Cryptococcus neoformans*. *Eukaryot. Cell* **1**, 432–439 (2002).
15. Shen, W. C., Davidson, R. C., Cox, G. M. & Heitman, J. Pheromones stimulate mating and differentiation via paracrine and autocrine signaling in *Cryptococcus neoformans*. *Eukaryot. Cell* **1**, 366–377 (2002).
16. Gyawali, R. et al. Pheromone independent unisexual development in *Cryptococcus neoformans*. *PLoS Genet.* **13**, e1006772 (2017).
17. Zhai, B. et al. Congenic strains of the filamentous form of *Cryptococcus neoformans* for studies of fungal morphogenesis and virulence. *Infect. Immun.* **81**, 2626–2637 (2013).
18. Wang, L. & Lin, X. Morphogenesis in fungal pathogenicity: shape, size, and surface. *PLoS Pathog.* **8**, e1003027 (2012).
19. Wang, L., Tian, X., Gyawali, R. & Lin, X. Fungal adhesion protein guides community behaviors and autoinduction in a paracrine manner. *Proc. Natl Acad. Sci. USA* **110**, 11571–11576 (2013).
20. Bassler, B. L. How bacteria talk to each other: regulation of gene expression by quorum sensing. *Curr. Opin. Microbiol.* **2**, 582–587 (1999).
21. Lee, H., Chang, Y. C., Nardone, G. & Kwonchung, K. J. *TUP1* disruption in *Cryptococcus neoformans* uncovers a peptide-mediated density-dependent growth phenomenon that mimics quorum sensing. *Mol. Microbiol.* **64**, 591–601 (2007).
22. Albuquerque, P. et al. Quorum sensing-mediated, cell density-dependent regulation of growth and virulence in *Cryptococcus neoformans*. *mBio* **5**, 13 (2013).
23. Homer, C. M. et al. Intracellular action of a secreted peptide required for fungal virulence. *Cell Host Microbe* **19**, 849–864 (2016).
24. Lin, X., Hull, C. M. & Heitman, J. Sexual reproduction between partners of the same mating type in *Cryptococcus neoformans*. *Nature* **434**, 1017–1021 (2005).
25. Wang, L. G. et al. Morphotype transition and sexual reproduction are genetically associated in a ubiquitous environmental pathogen. *PLoS Pathog.* **10**, e1004185 (2014).
26. Wang, L., Zhai, B. & Lin, X. The link between morphotype transition and virulence in *Cryptococcus neoformans*. *PLoS Pathog.* **8**, e1002765 (2012).
27. Goo, E., An, J. H., Kang, Y. & Hwang, I. Control of bacterial metabolism by quorum sensing. *Trends Microbiol.* **23**, 567–576 (2015).
28. Valbuena, N. & Moreno, S. AMPK phosphorylation by Ssp1 is required for proper sexual differentiation in fission yeast. *J. Cell Sci.* **125**, 2655–2664 (2012).
29. Esher, S. K., Granek, J. A. & Alspaugh, J. A. Rapid mapping of insertional mutations to probe cell wall regulation in *Cryptococcus neoformans*. *Fungal Genet. Biol.* **82**, 9–21 (2015).
30. Kim, D. E., Chivian, D. & Baker, D. Protein structure prediction and analysis using the Robetta server. *Nucleic Acids Res.* **32**, W526–W531 (2004).
31. Razin, S. V., Borunova, V. V., Maksimenko, O. G. & Kantidze, O. L. Cys2His2 zinc finger protein family: classification, functions, and major members. *Biochem. (Mosc.)* **77**, 217–226 (2012).
32. Nobile, C. J. et al. A recently evolved transcriptional network controls biofilm development in *Candida albicans*. *Cell* **148**, 126–138 (2012).
33. Alvaro, C. G. & Thorner, J. Heterotrimeric G protein-coupled receptor signaling in yeast mating pheromone response. *J. Biol. Chem.* **291**, 7788–7795 (2016).
34. Versele, M., Lemaire, K. & Thevelein, J. M. Sex and sugar in yeast: two distinct GPCR systems. *EMBO Rep.* **2**, 574–579 (2001).
35. Hsueh, Y. P., Xue, C. & Heitman, J. A constitutively active GPCR governs morphogenic transitions in *Cryptococcus neoformans*. *EMBO J.* **28**, 1220–1233 (2009).
36. Goodenough, U. & Heitman, J. Origins of eukaryotic sexual reproduction. *Cold Spring Harb. Perspect. Biol.* **6**, a016154 (2014).
37. Hsueh, Y. P., Xue, C. & Heitman, J. G protein signaling governing cell fate decisions involves opposing Galpha subunits in *Cryptococcus neoformans*. *Mol. Biol. Cell* **18**, 3237–3249 (2007).
38. White, J. M. & Rose, M. D. Yeast mating: getting close to membrane merger. *Curr. Biol.* **11**, R16–R20 (2001).
39. Horowitz, B. S., Zarnowski, R., Sharpee, W. C. & Keller, N. P. Morphological transitions governed by density dependence and lipoxygenase activity in *Aspergillus flavus*. *Appl. Environ. Microbiol.* **74**, 5674–5685 (2008).
40. Dumitru, R. et al. In vivo and in vitro anaerobic mating in *Candida albicans*. *Eukaryot. Cell* **6**, 465–472 (2007).
41. Chen, H. & Fink, G. R. Feedback control of morphogenesis in fungi by aromatic alcohols. *Genes Dev.* **20**, 1150–1161 (2006).
42. Honigberg, S. M. & Purnapatre, K. Signal pathway integration in the switch from the mitotic cell cycle to meiosis in yeast. *J. Cell Sci.* **116**, 2137–2147 (2003).
43. Fox, M. E. & Smith, G. R. Control of meiotic recombination in *Schizosaccharomyces pombe*. *Prog. Nucleic Acid. Res. Mol. Biol.* **61**, 345–378 (1998).
44. Feng, J. et al. GFOLD: a generalized fold change for ranking differentially expressed genes from RNA-seq data. *Bioinformatics* **28**, 2782–2788 (2012).
45. Skene, P. J. & Henikoff, S. A simple method for generating high-resolution maps of genome-wide protein binding. *eLife* **4**, e09225 (2015).

Acknowledgements

We thank P. Sharma and Wang laboratory members for critical reading, and S. Luo and H. Liu for their assistance in genetic screening. This work was financially supported by the National Science and Technology Major Project (2018ZX10101004), the Key Research Program of the Chinese Academy of Sciences (QYZDB-SSW-SSMC040), the Strategic Priority Research Program of the Chinese Academy of Sciences (XDPB03), the National Natural Science Foundation of China (Grants 31622004, 31570138, 31501008 and 31501009) and the National Institutes of Health (http://www.niaid.nih.gov/Pages/default.aspx) (R01AI097599 to X.L.). L.W. is a member of the Thousand Talents Program. X.L. holds an Investigator Award in the Pathogenesis of Infectious Disease from the Burroughs Wellcome Fund (http://www.bwfund.org/).

Author contributions

All authors contributed to the data analysis. X.T., G.-J.H., P.H., L.C., C.T., Y.-L.C., L.S., W.K., H.X., F.B., B.W., E.Y., X.L. and L.W. designed the experiments. X.T., G.-J.H. and P.H. conducted most of the studies. L.C. and E.Y. conducted most of the bioinformatics assays. Y.-L.C. and B.W. conducted the Rosetta ab initio and comparative modelling. L.S. conducted part of the overexpression plasmids construction. H.X. conducted the subcellular localization analysis. Y.Z. conducted part of the gene deletion experiments. Q.X., F.B., B.W., E.Y., X.L. and L.W. contributed reagents/materials/analysis tools. X.T., G.-J.H., X.L. and L.W. wrote the paper with contributions from all other authors.

Competing interests

The authors declare no competing interests.

Additional information

Supplementary information is available for this paper at https://doi.org/10.1038/s41564-018-0160-4.

Reprints and permissions information is available at www.nature.com/reprints.

Correspondence and requests for materials should be addressed to L.W.

Publisher's note: Springer Nature remains neutral with regard to jurisdictional claims in published maps and institutional affiliations.

nature research

Corresponding author(s): Linqi Wang

Life Sciences Reporting Summary

Nature Research wishes to improve the reproducibility of the work that we publish. This form is intended for publication with all accepted life science papers and provides structure for consistency and transparency in reporting. Every life science submission will use this form; some list items might not apply to an individual manuscript, but all fields must be completed for clarity.

For further information on the points included in this form, see Reporting Life Sciences Research. For further information on Nature Research policies, including our data availability policy, see Authors & Referees and the Editorial Policy Checklist.

Please do not complete any field with "not applicable" or n/a. Refer to the help text for what text to use if an item is not relevant to your study.
For final submission: please carefully check your responses for accuracy; you will not be able to make changes later.

Experimental design

1. Sample size

   Describe how sample size was determined.

   This is not relevant to the study. No statistical methods were used to predetermine samples sizes and no size calculation was performed prior to experimental design. We used 2-6 biological replicates for experiments as that is standard practice for most RNA-seq, genetic or microbiological assays.

2. Data exclusions

   Describe any data exclusions.

   No data were excluded

3. Replication

   Describe the measures taken to verify the reproducibility of the experimental findings.

   All experimental findings reported in the paper were reliably reproduced during replicate experiments.

4. Randomization

   Describe how samples/organisms/participants were allocated into experimental groups.

   This is not relevant to the study because specific genotype backgrounds were used for all the experiments and not applying a treatment to a larger subset of species.

5. Blinding

   Describe whether the investigators were blinded to group allocation during data collection and/or analysis.

   This is not relevant to the study because there was not group allocation in the study.

Note: all in vivo studies must report how sample size was determined and whether blinding and randomization were used.

6. Statistical parameters

   For all figures and tables that use statistical methods, confirm that the following items are present in relevant figure legends (or in the Methods section if additional space is needed).

n/a	Confirmed
☐	☒ The exact sample size (*n*) for each experimental group/condition, given as a discrete number and unit of measurement (animals, litters, cultures, etc.)
☐	☒ A description of how samples were collected, noting whether measurements were taken from distinct samples or whether the same sample was measured repeatedly
☐	☒ A statement indicating how many times each experiment was replicated
☐	☒ The statistical test(s) used and whether they are one- or two-sided *Only common tests should be described solely by name; describe more complex techniques in the Methods section.*
☒	☐ A description of any assumptions or corrections, such as an adjustment for multiple comparisons
☐	☒ Test values indicating whether an effect is present *Provide confidence intervals or give results of significance tests (e.g. P values) as exact values whenever appropriate and with effect sizes noted.*
☐	☒ A clear description of statistics including central tendency (e.g. median, mean) and variation (e.g. standard deviation, interquartile range)
☐	☒ Clearly defined error bars in all relevant figure captions (with explicit mention of central tendency and variation)

See the web collection on statistics for biologists for further resources and guidance.

Software

Policy information about availability of computer code

7. Software

Describe the software used to analyze the data in this study.	GraphPad Software 5.04, Rosetta 3.7, AxioCam MRm camera software Zen 2011, R statistical platform, MEGA(V5.04) and ImageJ (V2.1.4.7)

For manuscripts utilizing custom algorithms or software that are central to the paper but not yet described in the published literature, software must be made available to editors and reviewers upon request. We strongly encourage code deposition in a community repository (e.g. GitHub). *Nature Methods* guidance for providing algorithms and software for publication provides further information on this topic.

Materials and reagents

Policy information about availability of materials

8. Materials availability

Indicate whether there are restrictions on availability of unique materials or if these materials are only available for distribution by a third party.	There are no restrictions on material availability.

9. Antibodies

Describe the antibodies used and how they were validated for use in the system under study (i.e. assay and species).	Immunoprecipitation of mCherry-fused Cqs2 (ChromoTek RFP-Trap 70404002MA). It was validated by the manufacturers.

10. Eukaryotic cell lines

a. State the source of each eukaryotic cell line used.	No eukaryotic cell lines were used
b. Describe the method of cell line authentication used.	No eukaryotic cell lines were used
c. Report whether the cell lines were tested for mycoplasma contamination.	No eukaryotic cell lines were used
d. If any of the cell lines used are listed in the database of commonly misidentified cell lines maintained by ICLAC, provide a scientific rationale for their use.	No eukaryotic cell lines were used

Animals and human research participants

Policy information about studies involving animals; when reporting animal research, follow the ARRIVE guidelines

11. Description of research animals

Provide all relevant details on animals and/or animal-derived materials used in the study.	No animals were used

Policy information about studies involving human research participants

12. Description of human research participants

Describe the covariate-relevant population characteristics of the human research participants.	The study did not involve human research participants